CORROSIVENESS OF BIODIESEL OBTAINED FROM DIFFERENT RAW MATERIALS ON GRAY CAST IRON

EFECTOS CORROSIVOS DEL BIODIESEL EN LA FUNDICIÓN DE HIERRO GRIS A TEMPERATURA AMBIENTE

EFEITOS CORROSIVOS DO BIODIESEL NO FERRO FUNDIDO CINZENTO A TEMPERATURA AMBIENTE

José David Castro[1]*; Oscar Edwin Piamba[1] and Jhon Jairo Olaya[1]

[1] Grupo de Investigación en Corrosión, Tribología y Energía, Universidad Nacional de Colombia, Bogotá D.C.

e-mail: jodcastroca@unal.edu.co

ABSTRACT

The corrosive effects of biodiesel on gray cast iron at room temperature were studied. Static immersion tests were carried out through gravimetric techniques and in the absence of light, using five raw materials: beef tallow, lard, sunflower oil, soybean oil, and coconut oil. The influence of fatty acids that make up biodiesel was determined through linear regression with data obtained from the corrosion rate. Results show that biodiesels with a higher degree of unsaturated fats in their composition have a more significant effect on the loss of mass in the material, leading to more corrosive processes in gray cast iron.

*To whom correspondence should be addressed

RESUMEN

En esta investigación se estudian los efectos corrosivos del Biodiesel en la fundición de hierro gris a temperatura ambiente. Los ensayos de inmersión estática se realizaron mediante técnicas gravimétricas con ausencia de luz y con cinco diferentes materias primas: sebo vacuno, manteca de cerdo, aceite de girasol, aceite de soya y aceite de coco. La afectación de los ácidos grasos que componen los diferentes Biodiesel fue determinada por medio de la regresión lineal con los datos obtenidos de velocidad de corrosión. Los resultados muestran que el Biodiesel con mayor nivel de insaturación en su composición es el que afecta la pérdida de masa en el material de manera más significativa, llevando a procesos más corrosivos sobre la fundición gris.

Palabras clave: *Corrosión, Ácidos grasos, Biodiesel.*

RESUMO

Esta pesquisa estuda os efeitos corrosivos do Biodiesel no ferro fundido cinzento à temperatura ambiente. Os ensaios de imersão estática foram realizados mediante técnicas gravimétricas com ausência de luz e com cinco matérias primas diferentes: sebo bovino, gordura suína, óleo de girassol, óleo de soja e óleo de coco. O efeito dos ácidos graxos que compõem os diferentes Biodiesel foi determinado através da regressão linear com os dados avaliados da taxa de corrosão. Os resultados demonstram que os Biodiesel com maior concentração de ésteres insaturados afetam de forma mais significativa a perda de massa no material, causando processos mais corrosivos sobre o ferro fundido cinzento.

Palavras-chave: *Corrosão, Ácidos graxos, Biodiesel.*

1. INTRODUCTION

Given the growing demand for energy and the impending shortage of fossil fuels in the not too distant future, humanity has had to search for different renewable energy sources intended to ensure sustainable energy. One of the most widely used alternative fuels around the world is biodiesel. This is a renewable fuel known as acid alkyl ester obtained from animal (Amaya, Piamba, & Olaya, 2014) or vegetal sources. The raw materials used to produce biodiesel are commonly used in other fields or are waste products, which makes their production both inexpensive and feasible (Biodisol, 2014; Haseeb, Fazal, Jahirul, & Masjuki, 2011; Knothe, Gerpen, & Krahl, 2005). Most research on this fuel has been focused on its effects on the environment and the emissions into the atmosphere produced by combustion. For example, the methyl esters may serve as intermediaries in the production of fatty alcohols of vegetable oils. These alcohols have been used in surfactants and cleaning elements. Branched fatty acid esters have been used as lubricants, and their improved biodegradation makes them attractive in terms of their impact on the environment (Knothe *et al.*, 2005).

In the research area, the implementation of this new energy source has brought forward the need to understand the corrosion behavior of biodiesel when it comes in contact with the materials used with conventional diesel or when new production processes are implemented in industry, as is the case with fuel production. Corrosion is the degradation of a material that reacts with the surrounding environment. According to Nernst's theory, all metals have a tendency to become a solution. However, there has been progress in understanding the corrosive mechanism that acts on various materials, such as brass, copper, bronze, and carbon steel, among others (Fazal, Haseeb, & Masjuki, 2012; Haseeb *et al.*, 2011). The corrosion behavior that takes place during the interaction of biodiesel with some metal materials is associated with a degradation of biodiesel because of its hygroscopic properties (Fazal, Haseeb, & Masjuki, 2011; Fazal *et al*, 2012).

The biodiesel corrosion processes on metals are influenced by temperature, water content, microbial growth, and type of feedstock used to synthetize this fuel (Singh, 2012). The degradation of biodiesel includes an oxidative process, hydrolytic oxidation and microbiological activities. The oxidative process occurs when double and triple atomic bonds, preferably with a bis-allilyc bond configuration, react with the molecular oxygen, starting a chemical reaction of three stages. This chemical reaction produce peroxides, acids and aldehydes. The acids produced include formic, acetic and propionic acids, in addition to short fatty acid chains. These acids are highly corrosive on metals (Waynick, 2005). This reaction is increased by the catalytic effect of metals, however, some research studies show that the effect of the unsaturated bonds is predominant. (Christensen, 2014; McCormick, 2007; Knothe, 2007). The hydrolytic oxidation occurs by the presence of residual water in the biodiesel storage. The residual water can hydrolyze the biodiesel, producing free fatty acids and alcohol and increasing the acid number of biodiesel (da Silva, 2016; Aktas, 2010), while promoting the activities of microorganism into the fuel (Sorensen, 2011).

Gray cast irons are materials widely used in the automotive industry (Castiglioni, 2008) because of their low production costs and their high degree of mechanical resistance (ASTM International, 2013; Castiglioni, 2008). However, these materials exhibit chemical instability, which makes them prone to corrosive processes, thus affecting their service life. In various industries, this leads to increased maintenance costs for equipment fabricated with gray cast iron. This material has been used to fabricate blocks for diesel engines, spare parts for machinery, piping, valves, and supports (Callister, 2002; Castiglioni, 2008). Usually, engine parts made of this material are in direct contact with biodiesel.

Currently, the corrosion rate produced in a biodiesel environment is evaluated under the ASTM D130 standard, which measures the corrosion of a copper sheet. The procedure used with this standard involves immersing the sheet in the testing solution for a period of 3 hours with a constant temperature of 50 °C. The corrosion shown by the material is qualitatively evaluated through visual inspection according to the ASTM D130 standard, where 1A means the least impairment. However, this rule is of limited use in order to evaluate the corrosion of other materials or in the case of exposure to different fluids.

Moreover, Amaya, Piamba, & Olaya, (2014), carried out studies on the corrosive effects of palm biodiesel on gray cast iron at room temperature and cyclic oxidation. They reported an increase in the mass of the material until 48 hours of exposure, then the mass decreases until the end of the test. Also, it has been reported that the corrosion rates are four times higher if the metal-biodiesel interface is exposed to the cyclic oxidation test. According to data reported by Amaya *et al*. (2014), palm biodiesel has a higher degree of corrosiveness than conventional diesel.

Geller, Adams, Goodrum, & Pendergrass (2008), reported mass loss data in a corrosion test at room temperature, with 80:20 mixtures of poultry fat biodiesel-diesel, using different materials exposed for 7342 hours, including gray cast iron, with a loss of 0.03% with respect to its initial weight.

Fazal, Haseeb, & Masjuki, (2011). performed a comparison of different inhibitors added to palm biodiesel in order to improve the corrosion resistance of gray cast iron. They found a corrosion rate of 0.079 mpy (mils per year) when the material was exposed without inhibitors in the biodiesel. These tests were carried out in static immersion at 1200 hours and with room temperature exposure.

Fazal, Haseeb, & Masjuki (2012) showed the corrosiveness of palm biodiesel on copper, aluminum, brass, and cast iron through immersion at room temperature (25 °C – 27 °C) for 2880 hours. Reported corrosion rates were as follows: copper (0.39 mpy), brass (0.21 mpy), aluminum (0.17 mpy), and cast iron (0.11 mpy). Upon exposure of different metals to the biodiesel, they concluded that when copper and brass were exposed to the biodiesel, the TAN (total acid number) value increased, which is an indication of biodiesel degradation after the corrosion process. Nevertheless, they did not manage to relate another property with the corrosion.

Tsuchiya, Shiotani, Goto, Sugiyama, & Maeda (2006) conducted research on the corrosion process of fuel tank material in 5 % FAME (Fatty Acid Methyl Ester) blended diesel. The test was performed by immersion of the material at 80 °C in both corrosive media. After 500 hours of exposure, they reported corrosion pitting on the surface of the coupon that was exposed to 5 % FAME blended diesel. They were of the opinion that the TAN value was not high enough to explain the corrosion process. However, they suggested that the process of oxidation that took place reconverts esters into fatty acids.

Knothe & Dunn (2003) studied the behavior of the oil stability index applied to monoalkyl esters. In this study, the biodiesel composition and its contact with metals were considered. This exposure may affect the stability of the oxidation of biodiesel. The most representative factors that cause this behavior were the concentration of unsaturated fatty acids, the type of metal, and the molecular mass of the biodiesel.

Based on the results obtained in previous research, the present study aims to determine the corrosion resistance that occurs in cast iron when exposed to five types of biodiesel and to understand which components within the corrosive environment affect this process. The previous studies did not show a direct association between the fatty acids in the biodiesel and the corrosion process. The linear regression method was used to determine this relationship. This procedure allows for finding the linear correlation between two variables (one dependent and one independent) through the R^2 factor (if the factor is near to 1, the relationship between variables is strong) and determines whether the resulting behavior is statistically significant when using the F test (the F factor must be greater than its critical value for the test to be significant) in order to find the system equation (Cardona., González., Rivera, & Cárdenas, 2013). The technical standard ASTM G31, which describes the procedure, was used to conduct the immersion test. The material under study was characterized via optical microscopy, and its composition was determined through optical emission spectroscopy. The coupons of gray cast iron were weighted, and the data obtained were treated with linear regression, taking as the corrosion rate as dependent variable and the iodine index for each biodiesel as independent variable. The iodine index was calculated to determine the amount of unsaturation of fatty acids in the biodiesel. This index was calculated depending on the composition of each raw material and was useful to determine that the corrosion process shown in gray cast iron is linearly related to the unsaturation of each biodiesel when exposed at room temperature and in the absence of sunlight.

2. EXPERIMENTAL PROCEDURE

Preparation of Samples

Gray cast iron samples were obtained from parts of a repaired engine. Test coupons were cut down to a rectangular form of 18 mm × 18 mm × 7.5 mm. These cuts were performed using the wire-cut electrical discharge machining (EDM) technique, in order to avoid wasting material and also to maintain the microstructure as stable as possible.

After this process, coupons were treated as follows: polished with 80, 100, 240, 300, 600, 800, and 1200 sandpaper and with deionized water. Then the samples were polished with alumina until a mirror bright finish was achieved. Afterward, the pieces were cleaned for 10 minutes with ultrasound in acetone, isopropanol, and n-hexane. Finally, they were dried with compressed air and hot air.

Preparation of the Biodiesel

The Biodiesel production procedure in this test was based on the method presented by Piamba, 2009. The raw materials selected for the various corrosion tests were beef tallow, lard, coconut oil, soybean oil, and sunflower oil. The biodiesel was produced through the transesterification process, via methyl (Knothe, 2005). In order to produce the biodiesel, 500 mL of each raw material, 100 mL of anhydrous methanol (CH_3OH), and 1.75 g of sodium hydroxide (NaOH) flakes were used as a catalyst. First, each oil was dried at 100 °C for 15 minutes, using a 1000 mL Erlenmeyer flask and IKA ETS-D4 magnetic stirring. The sodium hydroxide was diluted in methanol in order to produce sodium methoxide. Then the oil temperature was lowered to 60 °C in the reactor without deactivating the stirrer. Sodium methoxide was carefully added to the oil, and the mixture was stirred for approximately 1 hour. Thereupon the solution was allowed to stand for 8 hours in a separate funnel at room temperature. The biodiesel was separated from the glycerol via decantation. Then the biodiesel was subject to three washing processes, using 150 mL of water each, and finally dried at 100 °C for 10 minutes.

Characterization

The surface of the metallic material was etched with Nital at 3.5 % vol and characterized via optical microscopy using a Leco brand image analyzer. The surface of the coupons was analyzed in magnification of 100X, 500X, 1000X, and 2000X. The ASTM A48M standard was used to determine the type of casting. Also, the chemical composition of the material was determined by means of the optical emission spectroscopy technique with Baird-Spectrovac 1000 equipment.

The evaluated properties of the corrosive environment are shown in Table 1.

Table 1. Properties and procedures used for biodiesel characterization.

Properties	Standard
Density at room temperature	ASTM D4052
Kinematic viscosity (40 °C)	ASTM D445
Molecular mass	N/A
Iodine index	N/A
Corrosion in Cu sheet	ASTM D130
Composition in fatty acids	N/A

The iodine index in the biodiesel was calculated using the Kyriakidis & Katsiloulis (2000) method with the following formula:

$$C_4 = xC_1 + yC_2 + zC_3 \tag{1}$$

Where, C4 is the iodine index and C1, C2, and C3 the concentrations of biodiesel classified as mono-unsaturated, bi-unsaturated, and tri-unsaturated, respectively. The variables x, y, and z were found by Kyriakidis & Katsiloulis (2000) to be 1, 1.5, and 2.62, respectively.

Gravimetric measurements

Before the corrosion test, the coupons were weighted on a Symmetry brand PA 220 digital scale with a resolution of 0.0001g. The quantity of coupons used for the test was 15. That means that for each Biodiesel 3 coupons were used. Subsequently, the samples, after being cut and polished, were immersed at room temperature (18 °C on average) and at atmospheric pressure (74.46 kPa) in a capsule of 316 L stainless steel with 20 mL of biodiesel and then sealed. After that, weight loss measurements were performed at

48-hour intervals until completing 450 hours of exposure. Before each measurement, the coupons were cleaned with ultrasound in acetone, isopropanol, and n-hexane. Also, they were dried with compressed air and then with hot air. Weight loss was calculated as the final percentage that the material lost with respect to the initial weight.

The corrosion rates in milli-inches per year (mpy) were based on ASTM G31, which allows to determine the weight lost, L, in kg, the density of the material, d, in kg/m^3, the area A in m^2, and the exposure time, t, in h, using the following *equation*:

$$\text{Corrosion rate } [mpy] = \frac{L \text{x} 3.46 \text{x} 10^6}{A \text{x} d \text{x} t} \qquad (2)$$

To show the influence on corrosion rate of the fatty acids that make up the various biodiesels in the biodiesel-gray iron system studied, the data obtained for the percentage of mass lost and the corrosion rate were subject to a linear regression analysis.

3. RESULTS AND DISCUSSION

Characterization of the material and the corrosive environment

Figure 1 shows a micrograph of gray cast iron without exposure to biodiesel. Based on the ASTM A48M standard, it was determined that the microstructure of the cast iron was type 30, due to presence of pearlite in the matrix and lamellar graphite type size 5.

Table 2 shows the results of the determination of the chemical composition using an optical emission spectrometer. The presence of C and Si at 3.45 % and 1.66 %, respectively, can be observed, which corresponds to a gray casting. Using the *Equation* (3), the carbon equivalent calculation (Bex, 1991) was 4 %, which classifies this material as hypoeutectic iron.
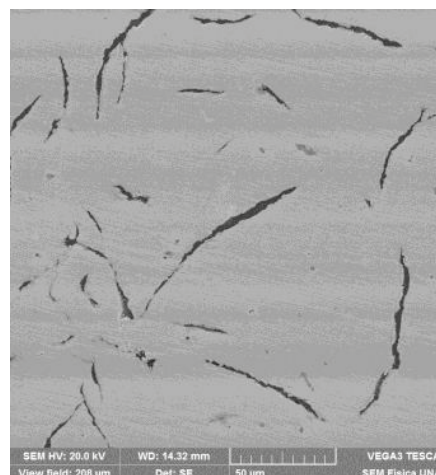

Figure 1. Micrograph of gray cast iron without biodiesel exposure. 2000X. Polished with alumina 10 μm. Lamellar graphite with perlitic phase in the matrix.

$$CE = \%C + 0.33(\%Si + \%P) = (.33 \text{ x } 1.66) + (.33 \text{ x } .02) \\ = 4.0044 \qquad (3)$$

In comparison with the composition of gray cast iron reported by the ASM Metals Handbook (ASM International, 1997), the material of this study is within the standard composition. Tables 3 and 4, show the properties and fatty acid composition of biofuels produced in the present study. It can be noted that biodiesels have different degrees of saturation. The saturated coconut oil biodiesel and the sunflower oil biodiesel are the most unsaturated.

Corrosive effects

Figure 2 shows the measurements of mass loss after the corrosion test compared to the initial weight of each specimen. It can be observed that after 450 hours of exposure, the sunflower biodiesel sample was the most affected, with a loss of approximately 0.030 % with respect to its initial weight. The sample corroded with soy biodiesel shows a similar behavior, and has a mass loss of about 0.025 %. Meanwhile, the gray cast iron exposed to coconut biodiesel shows a less aggressive behavior in this experiment.

Table 2. Chemical composition of gray cast iron using an optical emission spectrometer compared with standard composition (ASM International, 1997).

Material	Fe	C	Si	Mn	P
	% w/w	% w/w	% w/w	% w/w	% w/w
Gray cast iron coupons	93.41	3.45	1.66	0.66	0.02
Standard gray iron	-	2.5 - 4.0	1.0 - 3.0	0.2 - 1.0	0.002 - 1.0

Table 3. Properties of biodiesel obtained from different raw materials.

	Beef tallow	Lard	Soybean oil	Coconut oil	Sunflower oil
Density [g/mL] (21 °C)	0.8753	0.8750	0.8831	0.8525	0.8869
Kinematic viscosity [mm2/s] (40°C)	6.0373	5.3913	4.6323	3.5593	5.2073
Molecular mass [g/mol]	302.5	332.654	293.1	293.1	331.312
Iodine index	47.26	56.83	123.05	123.05	116.50
Corrosion in Cu Sheet	1a	1a	1a	1a	1a

Table 4. Composition of fatty acid radicals in percentages.

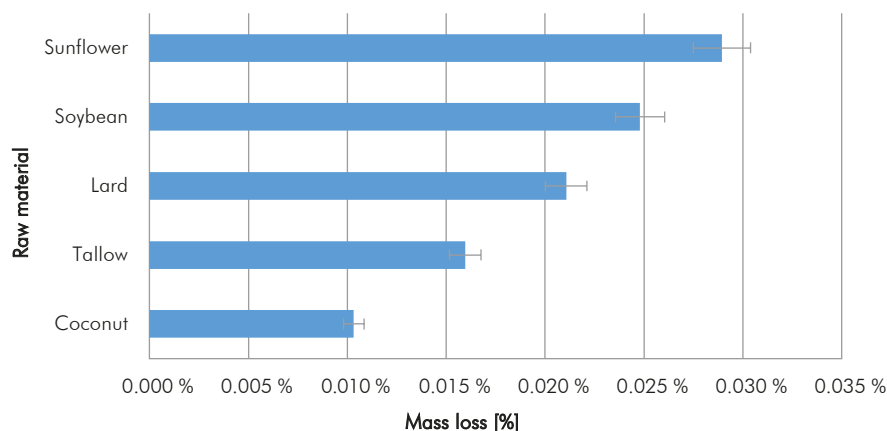|	Beef tallow	Lard	Soybean oil	Coconut oil	Sunflower oil
Lauric - 12:0	0.000	0.000	0.000	0.453	0.000
Myristic - 14:0	0.040	0.010	0.000	0.325	0.024
Palmitic - 16:0	0.274	0.280	0.116	0.119	0.032
Stearic - 18:0	0.256	0.130	0.032	0.017	0.063
Oleic - 18:1	0.391	0.460	0.204	0.033	0.470
Linoleic - 18:2	0.016	0.060	0.597	0.053	0.143
α-linolenic - 18:3	0.022	0.007	0.050	0.000	0.120

Figure 2. Graphic of percentage of total weight loss of the material for each biodiesel at room temperature.

Figure 3 shows the calculations of the corrosion rate that were obtained according to the ASTM G31 standard. It can be seen that the highest corrosion rate at 450 hours corresponds to the test performed with sunflower biodiesel, and the lowest corrosion rate pertains to the coco biodiesel test.

The first analysis seeks to identify whether there is a correlation between the size of the molecules of biodiesel and the corrosion rate. For this analysis, the value of the molecular mass for each type of biodiesel is used as an indicator of the size of the molecule. The second one evaluates the correlation between the
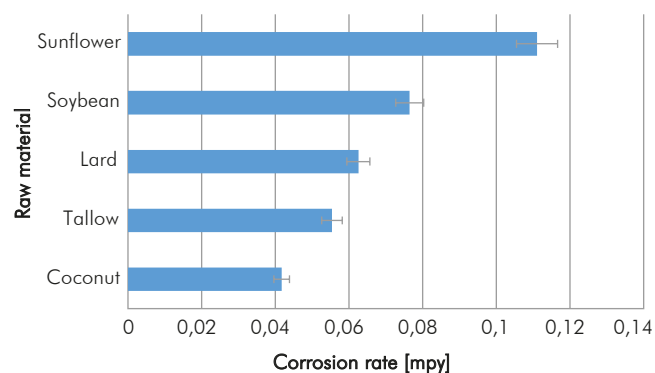
Figure 3. Graphic of corrosion rate in milli-inches per year (mpy) of the material for each biodiesel at room temperature.

corrosion rate and the composition of the biodiesel. This is expressed in terms of the iodine index as an indicator of the saturation of the ester chain.

Linear regression: "Corrosion rate vs. molecular weight"

The molecular mass is calculated from the concentration of radicals of fatty acids present in the esters of the biodiesel. The results obtained for each corrosive environment are shown in Table 3. The corrosion rate data and the molecular mass of the biodiesel were analyzed using the linear regression technique (Cardona *et al.*, 2013). The correlation results obtained are shown in Table 5.

Table 5. Coefficients obtained through linear regression: Corrosion velocity vs. molecular mass.

	Betas	Statistical Error Coefficient	Statistical t
Intercept	-3.33E-01	2.76E-01	-1.21E+00
Molecular mass	5.06E-03	9.16E-04	5.52E+00

Total sum of squares	2.003
R^2	0.160
Multiple correlation coefficient	0.470
F	3.676
Critical value of F	7.74E-02

Table 6. Coefficients obtained through linear regression: corrosion rate vs. iodine index.

	Betas	Statistical Error Coefficient	Statistical t
Intercept	6.58E-01	3.31E-02	1.98E+01
Iodine index	7.38E-03	4.00E-04	1.84E+01

Total sum of squares	2.003
R^2	0.974
Multiple correlation coefficient	0.862
F	37.474
Critical value of F	3.65E-05

The results of the linear regression analysis show a low correlation coefficient (R^2), which allows inferring that there is no trend or significant correlation between the size of molecules and the corrosion rate. This can also be inferred by comparing the values of the beta constants with the value of each constant statistical error, which are comparable in magnitude. Finally, it can be seen that the regression is statistically significant in terms of the values of F and its critical value (Cardona *et al.*, 2013).

Linear regression: "Rate of corrosion vs. iodine index"

Table 6 shows the results of the linear regression method linking the results of the corrosion rate and the iodine index.
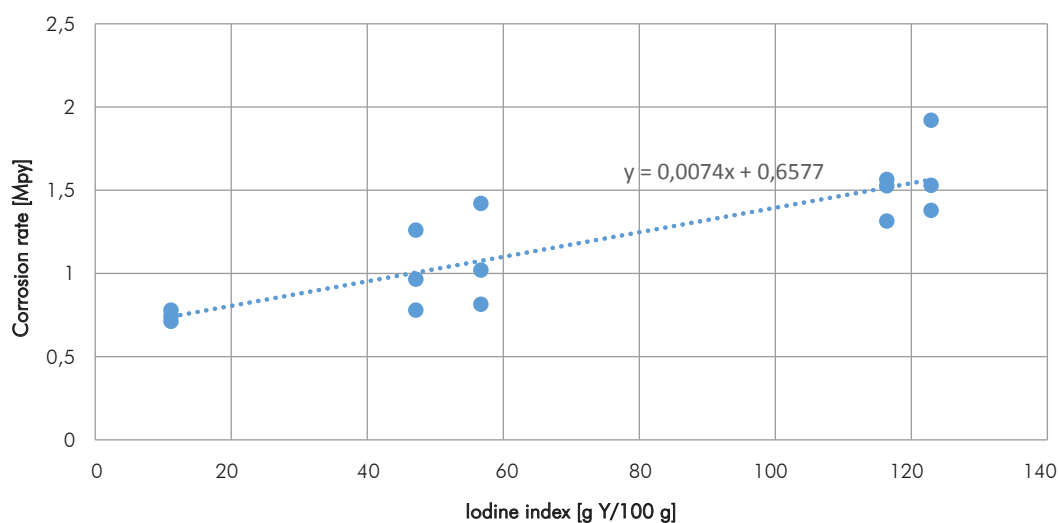

Figure 4. Measurements of the corrosion rate at room temperature and its linear regression

The results of the linear regression analysis show that the sample size used is sufficient for studying the correlation. The correlation coefficient R^2 was 0.97. The R^2 factor is close to 1, which allows us to infer that there is a trend and a significant relationship between the corrosion rate and the iodine index of the biodiesel. The statistical errors of every coefficient obtained are lower by an order of magnitude. This means that the approach made regarding the coefficients is close to the reality of the behavior of the corrosion rate. The linear regression is statistically significant because the F factor is greater than its critical value (Cardona *et al*., 2013), and therefore the number of coupons used was sufficient to show the corrosive effect over gray cast iron. Since the iodine concentration increases with the amount of unsaturated acid radicals in the composition of biodiesel, it can be seen that the corrosion rate becomes higher as the concentration of unsaturated fatty acids in the raw material increases. *Equation 4* shows the dependence of the corrosion rate on the Iodine index, as shown in Figure 4.

$$mpy = 6,58E\text{-}01 + 7,38E\text{-}03* \text{ iodine index} \qquad (4)$$

4. CONCLUSIONS

- The results show the corrosion observed in gray cast iron, using as parameters the following measurements of weight loss percentage and corrosion rates: Sunflower (0.029 %, 0.11 mpy), Soybean (0.025 %, 0.076 mpy), Lard (0.021 %, 0.062 mpy), Tallow (0.016 %, 0.05 mpy), and Coconut (0.010 %, 0.042 mpy). Linear regression analysis applied to the corrosion rate data shows that that there is no direct relationship with the size of the molecules, but it shows a significant relationship with the iodine index. By comparing these results with the iodine index of each raw material, it is possible to conclude that the composition of fatty acids is strongly linear related to the corrosion rate achieved in gray cast iron. Furthermore, the results show that biodiesel from oils with a higher content of unsaturated fatty acids have a greater effect on the corrosion process in gray cast iron.

ACKNOWLEDGEMENTS

REFERENCES

Amaya, A. A., Piamba, O., & Olaya, J. (2014). Estudio de los efectos corrosivos del diésel y biodiésel sobre una fundición de hierro gris. *R. Lat. Met. Mat.,* 34(2), 289-295.

Aktas, D., Lee, J., Little, B., Ray, R., Davidova, I., Lyles, C., & Suflita, J. (2010). Anaerobic metabolism of biodiesel and Its impact on metal corrosion. *Energ. Fuel.,* 24 (5), 2924-2928. DOI: 10.1021/ef100084j.

ASM International. (1997). ASM Metals Handbook Volume 1 - Properties and Selection: *Irons, steels, and high Perfomance alloys* (10th ed.). The materials information company.

ASTM A48 (2014). Gray Iron Castings, ASTM Corrosion of Metals; Wear and erosion, Volume 03.02, ASTM International, West Conshohocken, PA.

ASTM D130 (2015) Standard Test Method for Corrosiveness to Copper from Petroleum Products by Copper Strip Test, ASTM Petroleum Products, liquid fuels, and lubricants (I): C1234-D3710, Volume 05.01, ASTM International, West Conshohocken, PA.

ASTM G31 - Laboratory Immersion Corrosion Testing of Metals. ASTM Corrosion of Metals; Wear and Erosion, Volume 03.02, ASTM International, West Conshohocken, PA, 2014.

Bex, T. (1991). Chill testing: the effect of carbon equivalent. Mod. Cast., 83 (9), 59.

Biodisol. (2014). Energías alternativas, renovables, bioenergías.

Callister, W. (2002). *Introducción a la Ciencia e Ingeniería de los Materiales.* México: Reverté S.A.

Cardona M., D., González R., J., Rivera, M., & Cárdenas, E. (2013). Inferencia estadística Módulo de regresión lineal simple. Bogotá: Universidad del Rosario - Facultad de Administración.

Castiglioni, J. L. (2008). *In Materiales ferrosos y sus aplicaciones.,* Buenos Aires: Universidad de Buenos Aires.

Christensen, E., & McCormick, R. (2014). Long-term storage stability of biodiesel and biodiesel blens. *Fuel Process.* Technol., 128: 339-348.

Da Silva. W., Salomao, A., Vila, M., & Tubino, M. (2016). Influence of water and ultraviolet irradiation on the induction period of the oxidation of biodiesel. *J. Braz. Chem. Soc*., 28 (4), 676-680. DOI: 10.5935/0103-5053.20160201.

Fazal, M. A., Haseeb, A. S. M. A., & Masjuki, H. H. (2011). Effect of different corrosion inhibitors on the corrosion of cast iron in palm biodiesel. *Fuel Process. Technol*., 92(11), 2154–2159. http://dx.doi.org/10.1016/j.fuproc.2011.06.012.

Fazal, M. A., Haseeb, A. S. M. A., & Masjuki, H. H. (2012). Degradation of automotive materials in palm biodiesel. *Energy,* 40(1), 76–83. DOI: 10.1016/j.energy.2012.02.026.

Geller, D. P., Adams, T. T., Goodrum, J. W., & Pendergrass, J. (2008). Storage stability of poultry fat and diesel fuel mixtures: Specific gravity and viscosity. *Fuel*, 87(1), 92–102. DOI: http://dx.doi.org/10.1016/j.fuel.2007.03.043.

Grambow, B., & Revie, R. (2000). Uhlig´ s Corrosion Handbook. *Uhlig´ s Corrosion Handbook*. New Jersey: Wiley.

Haseeb, A. S. M. A., Fazal, M. A., Jahirul, M. I., & Masjuki, H. H. (2011). Compatibility of automotive materials in biodiesel: A review. *Fuel*, 90(3), 922–931.

Knothe, G., & Dunn, R. O. (2003). Dependence of oil stability index of fatty compounds on their structure and concentration and presence of metals. J. Amer. Oil Chem. Soc., 80(10), 1021–1026. DOI: 10.1007/s11746-003-0814-x.

Knothe, G., Gerpen, J. Van, & Krahl, J. (2005). *The Biodiesel Handbook*. United States: AOCS Press.

Knothe, G. (2007). Some aspects of biodiesel oxidative stability. *Fuel Process. Technol*., 88 (7), 669-677. DOI: http://dx.doi.org/10.1016/j.fuproc.2007.01.005.

Kyriakidis, N. B., & Katsiloulis, T. (2000). Calculation of iodine value from measurements of fatty acid methyl esters of some oils: Comparison with the relevant American oil chemists society method. *J. Amer. Oil Chem. Soc.*, 77(12), 1235–1238. DOI: 10.1007/s11746-000-0193-3.

McCormick, R., Ratcliff, M., Moens, L., & Lawrence, R. (2007) Several factors affecting the stability of biodiesel in standard accelerated test, *Fuel Process. Technol*., 88 (7), 651-657. DOI: http://dx.doi.org/10.1016/j.fuproc.2007..01.006.

Piamba, O. (2009). Estudo do desempenho do grupo motor-gerador alimentado com diferentes misturas diesel-biocombustíveis e avaliação de emissões. Tese de Doutorado Esc. De Engenharia, Universidade Federal Fluminense, Niterói, Brasil, 214pp.

Singh, B., Korstad, J., & Sharma, Y. C. (2012). A critical review on corrosion of compression ignition (CI) engine parts by biodiesel and biodiesel blends and its inhibition. *Renew. Sust. Energy Rev.*, 16(5), 3401–3408. DOI: http://dx.doi.org/10.1016/j.rser.2012.02.042.

Sorensen, G., Pedersen, D., Nørgaard, A., Sørensen, K., & Nygaard, S. (2011). Microbial growth studies in biodiesel blends. *Biores. Technol*., 102 (8), 5259–5264.

Tsuchiya, T., Shiotani, H., Goto, S., Sugiyama, G., & Maeda, A. (2006). Japanese Standards for diesel fuel containing 5% FAME: Investigation of acid generation in FAME blended diesel fuels and Its impact on corrosion. *SAE Techn. Papers Ser.* DOI: http://doi.org/10.4271/2006-01-3303.

Waynick, J. (2005) Characterization of Biodiesel Oxidation and Oxidation Products, Crc Project No. Avfl-2b. *National Renewable Energy Laboratory U.S. Department of Energy*.

AUTHORS

José David Castro.
Affiliation: *Grupo de investigación en Corrosión, Tribología y Energía. Universidad Nacional de Colombia.*
e-mail: jodcastroca@unal.edu.co

Oscar Edwin Piamba
Affiliation: *Grupo de investigación en Corrosión, Tribología y Energía. Universidad Nacional de Colombia.*
e-mail: oepiambat@unal.edu.co

Jhon Jairo Olaya.
Affiliation: *Grupo de investigación en Corrosión, Tribología y Energía. Universidad Nacional de Colombia.*
e-mail: jjolayaf@unal.edu.co